KJPP

Original Article

Deficiency of Anoctamin 5/TMEM16E causes nuclear positioning defect and impairs Ca^{2+} signaling of differentiated C2C12 myotubes

Tam Thi Thanh Phuong[#], Jieun An[#], Sun Hwa Park, Ami Kim, Hyun Bin Choi, and Tong Mook Kang*

Department of Physiology, Sungkyunkwan University School of Medicine, Suwon 16419, Korea

ABSTRACT Anoctamin 5 (ANO5)/TMEM16E belongs to a member of the ANO/TMEM16 family member of anion channels. However, it is a matter of debate whether ANO5 functions as a genuine plasma membrane chloride channel. It has been recognized that mutations in the ANO5 gene cause many skeletal muscle diseases such as limb girdle muscular dystrophy type 2L (LGMD2L) and Miyoshi muscular dystrophy type 3 (MMD3) in human. However, the molecular mechanisms of the skeletal myopathies caused by ANO5 defects are poorly understood. To understand the role of ANO5 in skeletal muscle development and function, we silenced the ANO5 gene in C2C12 myoblasts and evaluated whether it impairs myogenesis and myotube function. ANO5 knockdown (ANO5-KD) by shRNA resulted in clustered or aggregated nuclei at the body of myotubes without affecting differentiation or myotube formation. Nuclear positioning defect of ANO5-KD myotubes was accompanied with reduced expression of Kif5b protein, a kinesin-related motor protein that controls nuclear transport during myogenesis. ANO5-KD impaired depolarization-induced [Ca^{2+}]$_i$ transient and reduced sarcoplasmic reticulum (SR) Ca^{2+} storage. ANO5-KD resulted in reduced protein expression of the dihydropyridine receptor (DHPR) and SR Ca^{2+}-ATPase subtype 1. In addition, ANO5-KD compromised co-localization between DHPR and ryanodine receptor subtype 1. It is concluded that ANO5-KD causes nuclear positioning defect by reduction of Kif5b expression, and compromises Ca^{2+} signaling by downregulating the expression of DHPR and SERCA proteins.

INTRODUCTION

The Anoctamin (ANO)/TMEM16 family of plasma membrane proteins have been known to physiologically important for the regulation of ion transport, phospholipid scrambling, and other ionic conductance in numerous cell types [1]. Of those cloned 10 ANO family members (ANOs 1–10), ANO1 and ANO2 are the best-studied members that encode cytosolic Ca^{2+}-activated chloride channels (CaCC) and regulate vectorial epithelial transport, smooth muscle contraction, pain sensation, and cell proliferation [2,3]. However, the physiological functions and CaCC activity of other ANO family members (especially, ANOs 3–7) are still a matter of debate, because they reside mainly on the intracellular organellar membrane [4,5]. Among them, ANO5 is known to be highly expressed in bones, skeletal muscles, testes, and cardiac muscles [6].

In humans, autosomal dominant or recessive mutations in the ANO5 gene are related to bone fragility and muscular dystrophies with symptoms of muscular weakness and high plasma creatine kinase level [7,8]. Autosomal dominant ANO5 mutations are associated with gnathodiaphyseal dysplasia 1 (GDD1), with clinical symptoms of bone fragility and bony lesions of the jaw

bone [9]. Autosomal recessive ANO5 mutations are associated with muscular dystrophies limb girdle muscular dystrophy type 2L (LGMD2L) and Miyoshi muscular dystrophy type 3 (MMD3) [10-12]. Although ANO5-knockout (ANO5-KO) mice have been successfully produced recently, the phenotypes of the mice showed conflicting pathology in skeletal and cardiac muscles [6,13,14]. Therefore, the ANO5-KO mice model did not provide clearly the molecular mechanisms of skeletal myopathies caused by ANO5 deletion or genetic defects.

The development of skeletal muscle begins with the syncytial fusion of hundreds of myoblasts to form a very long myofiber [15]. In the process of skeletal muscle development or regeneration, nuclear movement along the length of myotube is required for evenly spaced nuclear positioning within the multinucleated long myofiber. It is also known that proper positioning of the nuclei is important for the functional capability of mature skeletal muscles, and disordered nuclear positioning is an indicator of myopathies such as centronuclear myopathies [15,16]. Nuclear migration and positioning are carried by the microtubule and microtubule-associated motor proteins (kinesins and dyneins) [15,16]. Among the motor proteins, Kif5b is a member of kinesin-related microtubule motor proteins that responsible for the axial movement of nuclei and mitochondria. Kif5b is highly expressed in skeletal muscles and responsible for the proper nuclear positioning and alignment in developing myotubes [15-18]. Even though the understanding of molecular mechanisms of nuclear positioning has evolved, it is not explored whether defected ANO5 is related to the mispositioning of myonuclei in differentiating muscle cells.

In the present in vitro study, we aimed to understand the cause of ANO5 defect-related myopathy and to explain the molecular functions of ANO5 by characterizing differentiation of ANO5-deficient C2C12 myoblasts. To the purpose, we silenced the ANO5 gene in C2C12 myoblasts by shRNA technique and tested whether it caused defects in myogenesis and excitation-contraction (E-C) coupling of the differentiated myotubes. ANO5 knockdown (ANO5-KD) did not greatly affect C2C12 myoblast differentiation. However, ANO5-KD caused nuclear positioning defect by the reduced expression of nuclear cargo protein Kif5b. ANO5-KD also suppressed Ca^{2+} signaling and E-C coupling efficiency of the myotubes by downregulating E-C coupling regulatory proteins.

METHODS

Cell culture

As we previously reported [19], murine C2C12 myoblasts (ATCC, Manassas, VA, USA) were cultured in high glucose DMEM (Gibco, Carlsbad, CA, USA) growth medium (GM) supplemented with 15% fetal bovine serum (FBS; Invitrogen, Carlsbad, CA, USA) and 1% penicillin-streptomycin (Gibco) at

37ºC with 5% CO_2. C2C12 myoblasts were plated in a 60 mm dish and then induced to differentiate into myotubes at 90%–100% confluence by replacing GM with differentiation medium (DM) supplemented with 2% horse serum (Gibco) for up to 3 days.

Stable knockdown of ANO5 in C2C12 myoblasts

Stable knockdown of ANO5 in C2C12 myoblasts was established by transfecting the shANO5 construct (pGFP-V-RS ANO5 shRNA cloning plasmid, OriGene Technologies, Rockville, MD, USA) by lipofectamine 2000 (Invitrogen). An shRNA target sequence for mouse Ano5 (accession number: NM_177694.6), 5'-AGGAGGCGTCTTATGTTCCAGAGAAGTGA-3', was selected using the OriGene shRNA design tool (construct #1 in Fig. 1A). The following forward and reverse oligonucleotides were synthesized: shANO5 (sense), 5'-gatccAGGAGGCGTCT-TATGTTCCAGAGAAGTGAtcaagagTCACTTCTCTGGAA-CATAAGACGCCTCCTtttttttggaaa-3'; shANO5 (antisense), 5'-tcgaaaaggtttttTCCTCCGCAGAATACAAGGTCTCTTCACT-gagaactAGTGAAGAGACCTTGTATTCTGCGGAGGAc-3'. After 48 h of shANO5 transfection, the cells were selected by treatment with 1 μg/ml puromycin for a week. The knockdown of ANO5 in stably transfected cells was confirmed by quantitative real-time RT-PCR and Western blot analysis.

Quantitative real time-PCR (qRT-PCR)

The qRT-PCR method was described in our previous report [19]. The primers used for the experiment were designed by a primer designing tool (NCBI) and were synthesized by Cosmo Genetech, Seoul, Korea. The following primers were used. Mouse Ano5 gene (NM_177694.6): forward primer: 5'-TACAGT-CACCGCCTGAGAAG-3', reverse primer: 5'-GACAAAGTC-GATCTGCCGGA-3', Kif5b gene (NM_008448.3): forward primer: 5'-GGAAGCCTTCACAGCGGATA-3', reverse primer: 5'-TGCTTGGAGGCGATTCAGTT-3'. The expressions of the genes were normalized with an internal control (tubulin). The relative mRNA value was calculated from Ct value by using the $2^{-\Delta\Delta CT}$ method for relative gene expression analysis.

Western blotting and antibodies

Cell samples for whole protein extraction were washed with PBS, and then lysed with RIPA buffer [25 mM Tris-HCl (pH 7.5), 1% Triton X-100, 0.5% sodium dedoxycholate, 140 mM NaCl, 1 mM MgCl₂, Halt protease inhibitor cocktail (EDTA-free)] (Pierce; Thermo Scientific, Waltham, MA, USA) on ice for 20 min. After that, the samples were centrifuged at 4°C for 15 min at 13,000 rpm. The supernatants were transferred to the new 1.5 ml tube and precipitations were discarded. Protein concentration in total lysates was measured by using the Bradford method with BSA standard curve. Whole protein (20 μg) was loaded per each lane
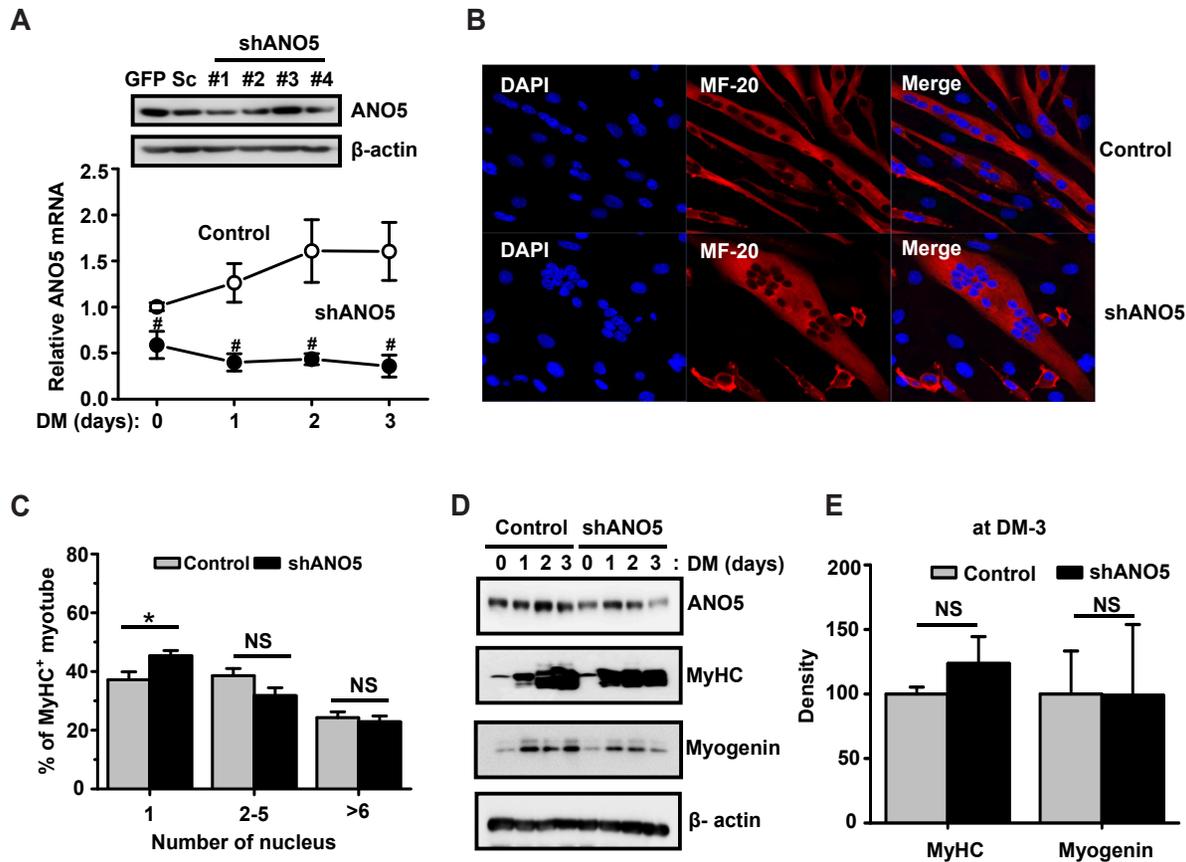
Fig. 1. ANO5 knockdown (ANO5-KD) impairs nuclear positioning without affecting myoblast differentiation. (A) The change of mRNA expression of ANO5 in control and ANO5-KD (shANO5) myoblasts during 3 days of differentiation period ($^\#p < 0.01$, 3 independent experiments). Inset: Knockdown efficiency of 4 shANO5 constructs (OriGene) tested were confirmed by Western blotting. The 'construct #1' shANO5 was chosen to generate stable ANO5-KD cells. (B) Representative immunostaining images of control and ANO5-KD myotubes after 3 days of differentiation. Shown are DAPI targeted myonuclei and anti-MF-20 targeted MyHC⁺ myotubes. (C) Bar graphs show the quantification of nuclei from (C) ($*p < 0.05$). (D) The expression of ANO5 and myogenic markers (MyHC and myogenin) in control and ANO5-KD cells at 3 days of differentiation (DM-3) was evaluated by Western blotting. (E) Bar graphs show the quantitative density of the myogenic marker protein bands (n = 5). GFP, green fluorescence protein; Sc, scrambled shRNA construct for control; MyHC, myosin heavy chain; NS, not significant.

in 6% or 8% polyacrylamide gel, 15 wells, 1.5 mm thickness. Then, proteins were transferred to Polyvinylidene difluoride (Carl Roth, Karlsruhe, Germany) and blocked with 5% skim milk (BD DIFCO, Sparks, MD, USA) then immunoblotted with indicated primary and secondary antibodies (Ab). At the final step, immunoblotted bands were detected by using an enhanced chemiluminescence (ECL) kit (Thermo Scientific). Abs against ANO5 was obtained from Arcis Biotechnology (Cheshire, UK), MF20 was obtained from R&D System (Minneapolis, MN, USA), Kif5b was obtained from ProSci Company (Poway, CA, USA). Abs against beta-actin, beta-tubulin, and C-myc were purchased from Sigma-Aldrich. Abs against ryanodine receptor 1 (RYR1) and dihydropyridine receptor (DHPR) were obtained from ThermoFisher Scientific (San Jose, CA, USA). Ab against SERCA-1 was obtained from Abcam (Cambridge, UK). Myogenin, calsequestrin-1, junctophilin-2, anti-rabbit and anti-mouse Abs were all obtained from Santa Cruz Biotechnology (Santa Cruz, CA, USA).

Immunocytochemistry and confocal imaging

The cells were fixed with 4% cold paraformaldehyde (Santa Cruz Biotechnology) for 15 min and then blocked by blocking buffer (1x PBS, 5% horse serum, and 0.3% Triton X-100) for 60 min. Fixed samples were incubated with anti-MF20 Ab (1:2,000) and anti-DHPR Ab (1:2,000) at 4°C overnight in anti-body dilution buffer (1x PBS, 1% BSA, and 0.3% Triton X-100), and then incubated with AlexaFlour dye at 488 nm and 647 nm (Invitrogen) for 1.5 h. After that, the nuclei of the cells were stained with DAPI for 15 min. The image acquisition was completed on confocal laser microscopy (LSM-710, Zeiss, Germany). Myotubes formation was assayed by counting the number of cells with mono-nucleus and multi-nuclei myosin heavy chain (MyHC)-positive (MyHC⁺) myotubes from five selected areas of three to five independent samples. Data were presented as the percentage of the cells that contained nucleus number of 1, 2–5, or ≥ 6 MyHC⁺ myotubes, as we previously described with modification [19]. To quantify the

nuclear positioning defect, we divided nuclear morphologies of MyHC$^+$ myotubes into 3 groups: (i) 'aligned' nuclei, (ii) 'aggregated' or clustered nuclei, and (iii) 'other' or mixed type of nuclei, as described in the previous study [20].

[Ca^{2+}]$_i$ measurements

C2C12 cells were plated in a thin glass coverslip and differentiated into myotube for 3 days in DM. The myotubes were loaded with 10 μM Fura 2-AM (Molecular Probe, Eugene, OR, USA) in an extracellular buffer solution containing (mM): 145 NaCl, 5 KCl, 1 MgCl$_2$, 10 HEPES, 10 glucose, and 1.5 CaCl$_2$ (pH 7.4 with NaOH) for 1 h at room temperature. After removing Fura-2 in supernatant, cells were subjected to perfusion chamber (RC-27NE2; Warner Instruments, Hamden, CT, USA) mounted on an inverted microscope (IX-70; Olympus, Tokyo, Japan). [Ca^{2+}]$_i$ was recorded with a ratiometric spectrofluorescence system (DeltaScan system; PTI, South Brunswick, NJ, USA) and emitted Fura-2 fluorescence ratios (F$_{340}$/F$_{380}$) was collected *via* a photomultiplier tube. Fluorescence signals were recorded and analyzed by Felix32 software (PTI), and the data were plotted as fluorescence ratio (F$_{340}$/F$_{380}$) and normalized to the [Ca^{2+}]$_i$ transient induced by treating the cells with 10 μM ionomycin (Biomol, Hamburg, Germany) at the end of each measurement. To compare depolarization-induced [Ca^{2+}]$_i$ transients, the single myotube was perfused briefly with high K$^+$ containing bath solution contained (mM): 100 KCl, 45 NaCl, 1 MgCl$_2$, 10 HEPES, 10 glucose and 1.5 CaCl$_2$ (pH 7.4 with NaOH). To estimate sarcoplasmic reticulum (SR) Ca^{2+} contents, the SR Ca^{2+} stores were depleted by rapid perfusion of bath solution containing 40 mM caffeine.

Statistics

Data were presented as mean ± standard deviation in qRT-PCR experiments and as mean ± standard error of mean in other experiments with the indicated numbers of experiments for each study. Data were analyzed using the Student's t-test, and p-values of < 0.05 were considered statistically significant.

RESULTS

ANO5-KD impairs nuclear positioning without affecting differentiation

To address the roles of ANO5 in C2C12 myoblast differentiation, we first measured ANO5 expression pattern (mRNA and protein) during the 3 days of differentiation period. In control C2C12 myoblasts, ANO5 mRNA (Fig. 1A) and proteins (Fig. 1D) gradually increased during the period of differentiation. Of those 4 tested shANO5 constructs (constructs #1-4; OriGene, Rockville, MD, USA), the 'construct #1' shANO5 was the most ef-

fective to knockdown ANO5 mRNA and protein expression (Fig. 1A, inset). Therefore, we have selected this shRNA construct to generate ANO5-KD myoblast cell line (see METHODS). During the differentiation of ANO5-KD myoblasts, ANO5 mRNA (Fig. 1A) and protein (Fig. 1D) expression remained lower levels than the control. Next, we investigated whether ANO5-KD affected C2C12 myoblast differentiation or myotube formation. As shown in Fig. 1B and C, ANO5-KD did not greatly suppress myotube formation, with a slightly lower percentage of MyHC$^+$ myotubes containing multiple nuclei (≥ 2 nuclei, differentiated) and a higher percentage of cells containing a single nucleus (undifferentiated myoblasts). The myotube formation was further quantified by immunoblotting of myogenic marker proteins, MyHC and myogenin (Fig. 1D). The quantified expression levels of these two marker proteins were similar between control and ANO5-KD cells (Fig. 1E). Taken together, these results indicate that ANO5 deficiency does not impair C2C12 myoblast differentiation or myotube formation.

However, we found the notable morphological differences between control and ANO5-KD myotubes. As clearly shown in Figs. 1B and 2A, multi-nucleated control myotubes were elongated and they have relatively even spaced nuclei that aligned along the myotube axis. On the contrary, ANO5-KD myotubes were much bigger or broader than control, and they had aggregated or clustered nuclei at the center of myotube cell body (Figs. 1B and 2A). We quantified the nuclear positioning defect of ANO5-KD myotubes by estimating the nuclear distribution pattern within each MyHC$^+$ myotube. As shown in Fig. 2B, ANO5-KD markedly increased the percentage of myotubes with aggregated nuclei (ANO5-KD 71.46 ± 3.9% *vs.* Control 16.4 ± 2.8%, p < 0.01), while the percentage of myotubes with aligned nuclei was significantly reduced in ANO5-KD (ANO5-KD 12.3 ± 2.33% *vs.* Control 72.04 ± 3.55%, p < 0.01). Disordered nuclear positioning of ANO5-KD myotubes was consistently observed over the entire shANO5 experiment. Taken together, these results suggest that ANO5 deficiency leads to impairment of proper nuclear positioning in the process of C2C12 myoblast differentiation.

ANO5-KD downregulates expression of Kif5b motor protein during myogenesis

We examined whether ANO5-KD affected the expression of Kif5b, a nuclear motor protein. Immunostaining of Kif5b in differentiated myotubes showed that Kif5b proteins are located throughout the cytoplasm of both groups of cells, while the aggregated nuclei were clearly visible only in ANO5-KD cells (Fig. 2A). To examine the relationship between the ANO5-KD-induced nuclear positioning defect and the expression of Kif5b, the mRNA and protein expression levels of Kif5b were quantified during the differentiation period. In control cells, Kif5b mRNA (Fig. 2C) and proteins (Fig. 2D) gradually increased during the period of differentiation. In ANO5-KD cells, the significantly reduced Kif5b
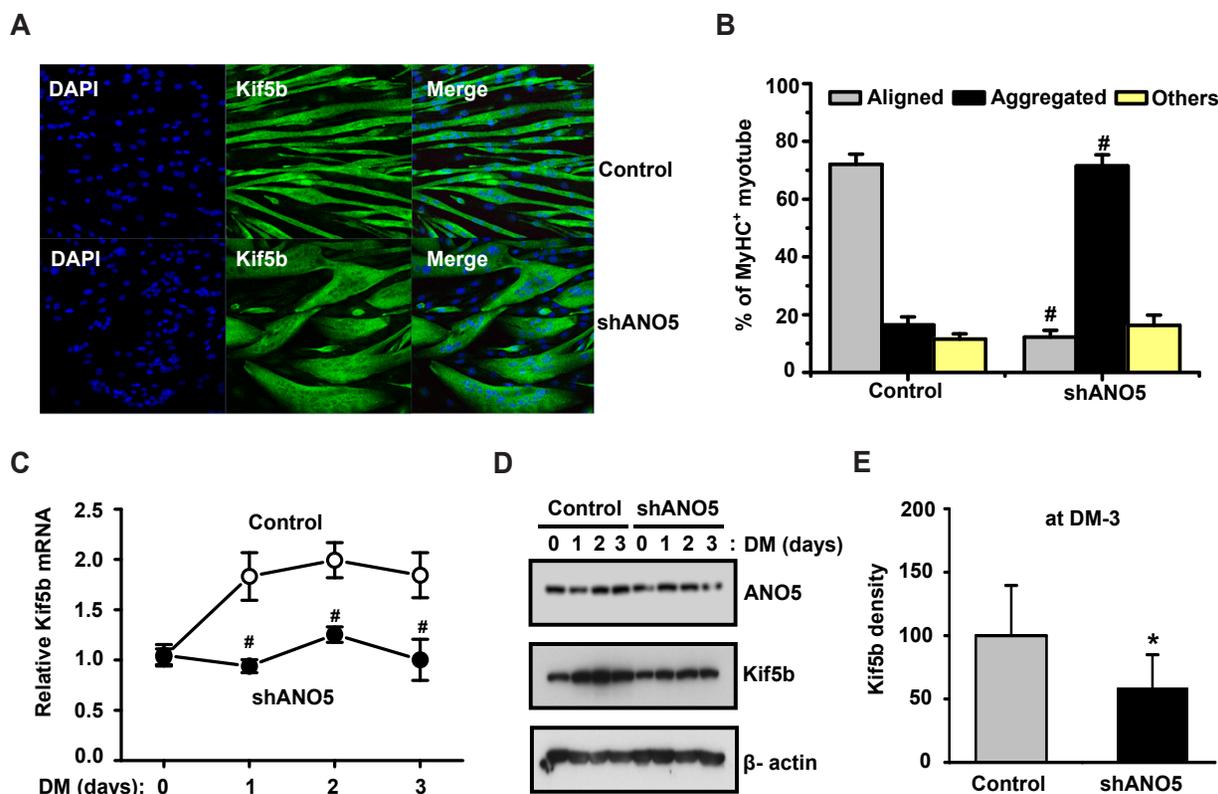
Fig. 2. ANO5 knockdown (ANO5-KD) causes nuclear positioning defect and reduced expression of Kif5b nuclear motor proteins. (A) Representative DAPI and anti-Kif5b immunostaining images were taken from control and ANO5-KD myotubes after 3 days of differentiation. ANO5-KD myotubes showed aggregated or clustered nuclei at the center of the cell body. (B) The degree of nuclear positioning defect was evaluated by counting the percentage of myotubes with nuclei of 'aligned', 'aggregated', and 'other' mixed type (n = 5, #p < 0.01). (C, D) The changes in Kif5b mRNA expression (#p < 0.01, n = 3) and Kif5b protein expression during 3 days of myogenesis were illustrated. (E) Kif5b protein expression levels at DM-3 were quantified and compared between two groups (*p < 0.05, n = 3). MyHC, myosin heavy chain; DM, differentiation medium.

mRNA (Fig. 2C) and protein (Fig. 2D) expression levels remained constant during differentiation. Nonetheless, it is of note that ANO5-KD does not suppress expression levels of Kif5b mRNA and proteins at the beginning of differentiation (at DM0 in Fig. 2C and D). In ANO5-KD myotubes after 3 days of differentiation (DM3), the normalized Kif5b protein expression level was significantly lower than the control (~50% of control, p < 0.05; Fig. 2E). These data suggest that nuclear positioning defect of the ANO5-KD myotubes is closely related to the reduced expression of Kif5b in the course of differentiation. We performed immunostaining of some microtubule molecules such as alpha- and beta-tubulins to see whether their organization is disorganized by ANO5 deficiency. However, the distribution of the microtubule molecules was not altered by ANO5-KD (data not shown).

ANO5-KD compromises Ca²⁺ signaling

To evaluate the functional impact of the ANO5-KD that causes clustered nuclei, we compared the Ca²⁺ signaling of the myotubes. Depolarization-induced $[Ca^{2+}]_i$ transients was repeatedly recorded by brief perfusion of 100 mM K⁺-containing bath solution. Although the resting $[Ca^{2+}]_i$ levels were similar between two groups,

normalized amplitudes of the $[Ca^{2+}]_i$ transients in ANO5-KD myotubes were ~30% smaller than the control (Fig. 3A, B). We next examined whether the weak Ca²⁺ response to depolarization is caused by reduced SR Ca²⁺ storage or contents. The SR Ca²⁺ stores were depleted with 40 mM caffeine, and the experiment revealed that the amounts of SR Ca²⁺ released from the ANO5-KD myotubes were ~30% less than control cells (Fig. 3C, D). These Ca²⁺ experiments suggest that ANO5-KD reduces E-C coupling efficiency mainly by the reduction of SR Ca²⁺ storage, which can be caused by insufficient Ca²⁺ reuptake by the SERCA pump.

ANO5-KD reduces expression of DHPR and SERCA and impairs co-localization of DHPR and RyR1

We next questioned whether the reduced E-C coupling efficiency or Ca²⁺ signaling of ANO5-KD cells is related with reduced expression of E-C coupling regulatory proteins. The Western blotting analysis showed that expression of DHPR and SERCA proteins are significantly reduced in ANO5-KD myotubes, while the expression levels of RYR1, calsequestrin-1, and junctophilin-2 are not changed (Fig. 4A, B). These results suggested that the reduced Ca²⁺ transients and less SR Ca²⁺ release observed in ANO5-
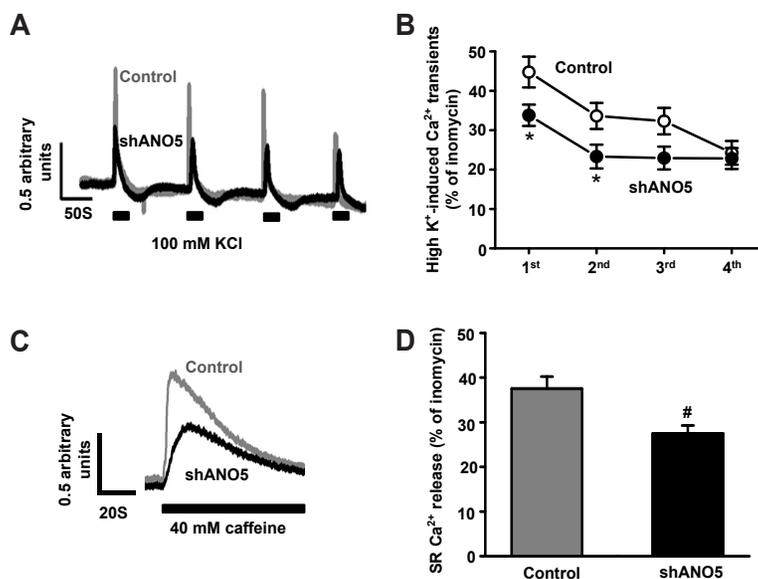
Fig. 3. ANO5 knockdown (ANO5-KD) compromises Ca²⁺ signaling. (A) Representative [Ca²⁺]ᵢ transients that evoked by 100 mM KCl-induced membrane depolarization (high-K solution). Control (n = 24) and ANO5-KD myotubes (n = 17) were repeatedly depolarized at every ~2 min. (B) The line graph shows the quantitated and normalized Ca²⁺ transients (*p < 0.05). (C) Representative sarcoplasmic reticulum (SR) Ca²⁺ releases in response to the perfusion of 40 mM caffeine to deplete SR Ca²⁺ stores. (D) The areas under the Ca²⁺ release curves were calculated, normalized, and illustrated as bar graphs (#p < 0.01).
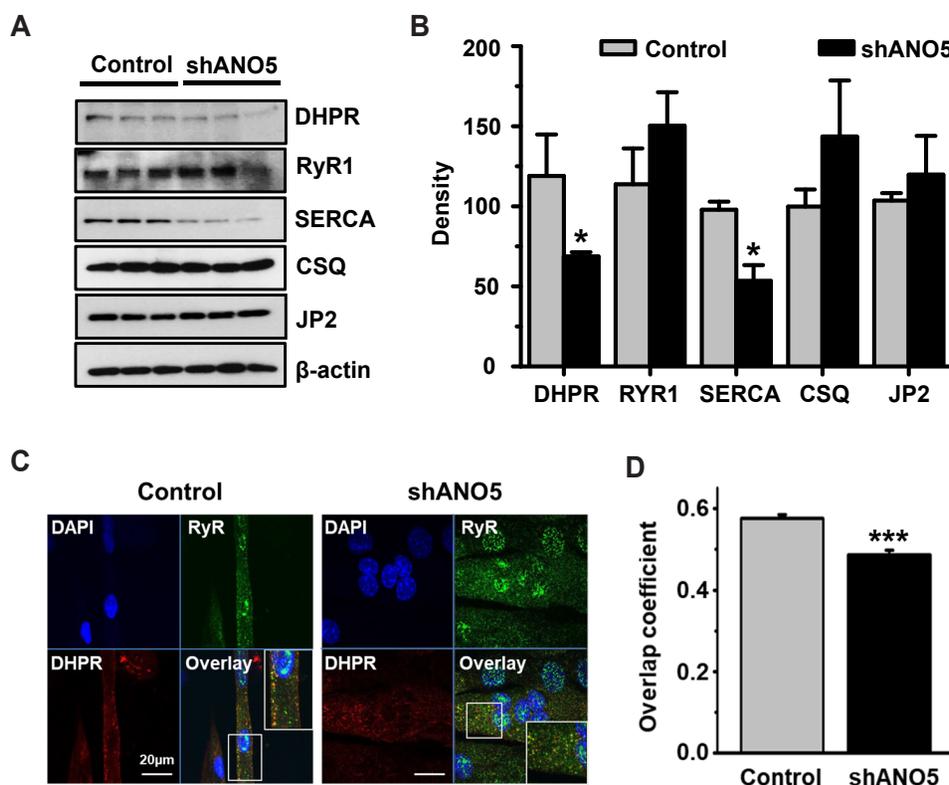

Fig. 4. ANO5 knockdown (ANO5-KD) reduces expression of DHPR and SERCA and impairs co-localization of dihydropyridine receptor (DHPR) and ryanodine receptor subtype 1 (RyR1). (A) The expression of E-C coupling regulatory proteins was compared between control and ANO5-KD myotubes. Western blotting was performed with myotubes harvested at differentiation medium (DM)-3. (B) The quantified protein expression levels were illustrated as bar graphs, showing that DHPR and SERCA expression is reduced by ANO5-KD (*p < 0.05). (C) The myotubes at DM-3 were immunostained against RyR1 and DHPR, and the co-localization of the two proteins was analyzed by calculating overlap coefficient. (D) The calculated overlap coefficient was compared with the bar graph (***p < 0.005). CSQ, calsequestrin-1; SERCA, SR Ca²⁺-ATPase; JP2, junctophilin-2.

KD cells (Fig. 3) are caused by impaired expression of membrane voltage sensor (DHPR) and SR Ca²⁺ reuptake pump (SERCA).

In addition to the reduced protein expression of DHPR, confocal image analysis of the immunostained myotubes revealed that the co-localization between DHPR and RyR1 has impaired by ANO5 deficiency. DHPR proteins of the control myocytes were highly localized to the cell periphery or cell membrane, while DHPRs of the ANO5-KD were localized throughout the myotube (Fig. 4C). Nonetheless, the superposition or co-localization of DHPR and RyR1 in ANO5-KD cells was not as low as we have expected. As a result, the quantified overlap coefficient value of the ANO5-KD myotubes was reduced to 84% of the control myotubes (p < 0.005; Fig. 4D). Since direct mechanical coupling between the DHPR and RyR1 is strictly required for depolarization-induced gating of SR RyR1 Ca²⁺ release channels, the impaired or reduced DHPR-RyR1 coupling explains, in part, why the depolarization-induced Ca²⁺ transients were diminished in the ANO5-KD cells (Fig. 3). Taken together, reduced Ca²⁺ signaling and E-C coupling efficiency of the ANO5-KD myotubes were explained both by the reduced expression of DHPR and SERCA and the impaired coupling between DHPR and RyR1.

DISCUSSION

Our study found that ANO5 knockdown does not impair C2C12 myogenesis, but the ANO5-KD myotubes showed impaired nuclear positioning and Ca²⁺ signaling. The mispositioning of myonuclei in ANO5-KD myotubes was accompanied with reduced protein expression of Kif5b, DHPRs, and SERCA. The aggregated myonuclei in ANO5-KD myotubes are closely related with the suppressed expression of Kif5b during myogenesis. The compromised Ca²⁺ transient to depolarization can be explained by the reduced expression of DHPR and SERCA, and in part by the impaired co-localization between DHPR and RyR1.

Our results show that ANO5-KD myotubes were much bigger or broader than control, and they have aggregated or clustered myonuclei at the center of myotube (Figs. 1B and 2A). Since the expression of myofusion markers and the proportion of multinucleated MyHC⁺ cells are similar between two groups (Fig. 1), abnormal morphology of ANO5-KD myotubes can be attributed to the dysfunction of nuclear positioning. The aggregated myonuclei were accompanied with lower protein expression of Kif5b (Fig. 2D). Kif5b is a microfilament-associated motor protein that responsible for the axial movement of myonuclei in differentiating muscle cells *in vivo* and *in vitro* [15-18]. Kif5b associates with microtubule-associated protein 7 (MAP7) which was found to be important for nuclear positioning during the development of drosophila skeletal muscles and C2C12 skeletal myotubes [16]. In our study, ANO5-KD cells expressed less Kif5b, and the reduced expression remained low during myoblast differentiation period. However, undifferentiated ANO5-KD myoblasts expressed Kif5b

similar to the control level at DM0 (DM0 myoblasts of > 90% confluence). Therefore, it suggests that ANO5 silencing does not directly inhibit gene expression of Kif5b in C2C12 cells. The fact that Kif5b expression of ANO5-KD cells is not able to increase during the differentiation period indicates that Kif5b expression begins to increase as the cells differentiate under the guidance of ANO5. For this reason, a lack of ANO5 will lead to the failure of Kif5b-dependent nuclear positioning and alignment. Another plausible explanation is that ANO5 deficiency causes inappropriate myofusion that results in the failure of proper elongation of the developing myotube. If ANO5-KD myoblasts failed to elongate, the cells would be juxtaposed to each other to make a broad-shaped myotubes and the nuclei will be aggregated into a specific site of the muscle cell. Although the endoplasmic reticulum (ER) expression of ANO5 has been reported, its functional relevance is largely unknown [5,21]. If ANO5 on the ER membrane regulates ER stress response, ANO5 deficiency can lead to a change of gene expression that responsible for nuclear positioning during myogenic development. Previous studies showed that some genetic mutations of ANO5 results in centered nuclei in human skeletal muscles [10,22]. Therefore, our findings are in accordance with these reports on the Kif5b-associated mispositioning of myonuclei and the ANO5-mutants causing human muscle symptoms. Our findings of the nuclear positioning defect and impaired Ca²⁺ signaling in ANO5-deficient C2C12 myotubes are in accordance with pathological phenotypes found in ANO5-KO mice model [13]. The histological evaluation of the ANO5-KO mouse skeletal muscles exhibited central myonuclei, cytoplasmic aggregation, and necrotic muscle fibers. Functional analysis showed the ANO5-KO muscles have reduced repair capacity to membrane injury, and defective myofusion necessary for the muscle repair and regeneration. In addition, the contractile forces of the diaphragm was significantly decreased by ANO5 deficiency [13]. Overall, this ANO5-KO mouse model recapitulates adult-onset of LGMD2L of humans. However, our findings are inconsistent with the findings from another ANO5-KO mice model, in which genetic deletion of ANO5 does not recapitulate human ANO5 defects and related muscular pathology [6]. In addition, the ANO5-KO mice did not show defects in nuclear positioning and muscle functions [6]. At present, it is difficult to explain the reason for differences between the ANO5-KO mice results and our *in vitro* findings with C2C12 cells. Therefore, a more definitive experiment should be carried out to explain these differences.

ANO5-KD results in reduced expression of DHPR and SERCA proteins (Fig. 4), by which the depolarization-induced Ca²⁺ transients were decreased by ~30% (Fig. 3). Skeletal muscle contraction is mediated by SR Ca²⁺ release that is mediated by DHPR activation of RyR1 Ca²⁺ channel opening. In our ANO5-KD cell study, the amplitudes of Ca²⁺ transients (~70% of control) were matched well with the reduced amounts of SR Ca²⁺ release or SR contents (~70% of control). This explains that compromised Ca²⁺ signaling of the ANO5-KD cells is mainly derived by the re-

duced SERCA activity and SR Ca^{2+} storage. The reduced SERCA expression limits SR Ca^{2+} reuptake and consequently reduces SR Ca^{2+} contents. Additionally, mismatched molecular localization of DHPR and RyR1 can be an additional reason for the compromised Ca^{2+} signaling, because their direct interaction is strictly required for E-C coupling (Fig. 4). The reduced expression of plasma membrane DHPR can impair not only the voltage sensing of membrane depolarization but also mechanical transduction to open RyR1 channels on the SR membrane. Taken together, all of these disorders combine to eventually reduce the E-C coupling efficiency of the ANO5-KD myotubes.

ANO5 has been known to be expressed mainly in the ER membrane unless ANO5 is heterogeneously overexpressed [14]. Previous report showed that HEK-293 or myocyte overexpression system can express ANO5 proteins on the cell surface membrane [13,23]. Even if ANO5 is overexpressed in HEK cells or myocytes, only a small fraction of the ANO5 protein was found in the cell membrane, in which ANO5 can play as a non-selective ion channel and a Ca^{2+}-dependent phospholipid scramblase [14]. However, their data clearly showed that the major population of ANO5 proteins is located in the intracellular membrane such as the ER membrane. If ANO5 is expressed on the plasma membrane of native myocytes, it can work as Ca^{2+}-dependent phospholipid scramblase and non-selective ion channel [14,23]. Assuming that ANO5 is expressed highly in the plasma membrane of C2C12 myoblasts and acknowledging a pivotal role of the plasma membrane potential, raised Ca^{2+}, and extracellular exposure of phosphatidylserine in the process of myoblast fusion [13,14,23,24], we can speculate that ANO5 deficiency impairs greatly the myofusion or myotube formation in our ANO5-KD C2C12 cells. However, differentiation or myotube formation of the ANO5-KD cells was comparable to the control cells (Fig. 1), suggesting the minor role, if any, of the plasma membrane-localized ANO5 in the fusion process. Therefore, we acknowledge that the functions of ANO5 as a plasma membrane channel and/or phospholipid scramblase are still under debate. Most of the ANO5 proteins are localized in the ER membrane, where it can regulate ER luminal Ca^{2+} levels and cytosolic Ca^{2+} levels [21]. Supporting the ER localization of ANO5, we found that ANO5-KD myotubes show considerably attenuated SR Ca^{2+} release in response to caffeine, suggesting the reduced ER Ca^{2+} storage by deficiency of ANO5. In our study, the defect in nuclear positioning of ANO5-KD myotubes can result from the impaired Ca^{2+}-dependent cellular pathways that compromise the organization of the nucleoskeleton or cytoskeleton. However, understanding precise molecular mechanisms underlying functional coupling between ANO5 and myonuclear positioning and alignment requires more in-depth studies.

CONFLICTS OF INTEREST

The authors declare no conflicts of interest.

REFERENCES

1. Pedemonte N, Galietta LJ. Structure and function of TMEM16 proteins (anoctamins). *Physiol Rev.* 2014;94:419-459.
2. Yang YD, Cho H, Koo JY, Tak MH, Cho Y, Shim WS, Park SP, Lee J, Lee B, Kim BM, Raouf R, Shin YK, Oh U. TMEM16A confers receptor-activated calcium-dependent chloride conductance. *Nature.* 2008;455:1210-1215.
3. Stephan AB, Shum EY, Hirsh S, Cygnar KD, Reisert J, Zhao H. ANO2 is the cilial calcium-activated chloride channel that may mediate olfactory amplification. *Proc Natl Acad Sci U S A.* 2009;106:11776-11781.
4. Tian Y, Schreiber R, Kunzelmann K. Anoctamins are a family of Ca^{2+}-activated Cl- channels. *J Cell Sci.* 2012;125(Pt 21):4991-4998.
5. Duran C, Qu Z, Osunkoya AO, Cui Y, Hartzell HC. ANOs 3-7 in the anoctamin/Tmem16 Cl- channel family are intracellular proteins. *Am J Physiol Cell Physiol.* 2012;302:C482-493.
6. Xu J, El Refaey M, Xu L, Zhao L, Gao Y, Floyd K, Karaze T, Janssen PM, Han R. Genetic disruption of Ano5 in mice does not recapitulate human ANO5-deficient muscular dystrophy. *Skelet Muscle.* 2015;5:43.
7. Bouquet F, Cossée M, Béhin A, Deburgrave N, Romero N, Leturcq F, Eymard B. Miyoshi-like distal myopathy with mutations in anoctamin 5 gene. *Rev Neurol* (*Paris*). 2012;168:135-141.
8. Penttilä S, Palmio J, Suominen T, Raheem O, Evilä A, Muelas Gomez N, Tasca G, Waddell LB, Clarke NF, Barboi A, Hackman P, Udd B. Eight new mutations and the expanding phenotype variability in muscular dystrophy caused by ANO5. *Neurology.* 2012;78:897-903.
9. Tsutsumi S, Kamata N, Vokes TJ, Maruoka Y, Nakakuki K, Enomoto S, Omura K, Amagasa T, Nagayama M, Saito-Ohara F, Inazawa J, Moritani M, Yamaoka T, Inoue H, Itakura M. The novel gene encoding a putative transmembrane protein is mutated in gnathodiaphyseal dysplasia (GDD). *Am J Hum Genet.* 2004;74:1255-1261.
10. Hicks D, Sarkozy A, Muelas N, Köehler K, Huebner A, Hudson G, Chinnery PF, Barresi R, Eagle M, Polvikoski T, Bailey G, Miller J, Radunovic A, Hughes PJ, Roberts R, Krause S, Walter MC, Laval

SH, Straub V, Lochmüller H, Bushby K. A founder mutation in Anoctamin 5 is a major cause of limb-girdle muscular dystrophy. *Brain*. 2011;134(Pt 1):171-182.

11. Little AA, McKeever PE, Gruis KL. Novel mutations in the Anoctamin 5 gene (ANO5) associated with limb-girdle muscular dystrophy 2L. *Muscle Nerve*. 2013;47:287-291.

12. Bolduc V, Marlow G, Boycott KM, Saleki K, Inoue H, Kroon J, Itakura M, Robitaille Y, Parent L, Baas F, Mizuta K, Kamata N, Richard I, Linssen WH, Mahjneh I, de Visser M, Bashir R, Brais B. Recessive mutations in the putative calcium-activated chloride channel Anoctamin 5 cause proximal LGMD2L and distal MMD3 muscular dystrophies. *Am J Hum Genet*. 2010;86:213-221.

13. Griffin DA, Johnson RW, Whitlock JM, Pozsgai ER, Heller KN, Grose WE, Arnold WD, Sahenk Z, Hartzell HC, Rodino-Klapac LR. Defective membrane fusion and repair in Anoctamin5-deficient muscular dystrophy. *Hum Mol Genet*. 2016;25:1900-1911.

14. Whitlock JM, Yu K, Cui YY, Hartzell HC. Anoctamin 5/TMEM16E facilitates muscle precursor cell fusion. *J Gen Physiol*. 2018;150:1498-1509.

15. Gache V, Gomes ER, Cadot B. Microtubule motors involved in nuclear movement during skeletal muscle differentiation. *Mol Biol Cell*. 2017;28:865-874.

16. Metzger T, Gache V, Xu M, Cadot B, Folker ES, Richardson BE, Gomes ER, Baylies MK. MAP and kinesin-dependent nuclear positioning is required for skeletal muscle function. *Nature*. 2012; 484:120-124.

17. Wilson MH, Holzbaur EL. Opposing microtubule motors drive robust nuclear dynamics in developing muscle cells. *J Cell Sci*. 2012; 125(Pt 17):4158-4169.

18. Wang Z, Cui J, Wong WM, Li X, Xue W, Lin R, Wang J, Wang P, Tanner JA, Cheah KS, Wu W, Huang JD. Kif5b controls the localization of myofibril components for their assembly and linkage to the myotendinous junctions. *Development*. 2013;140:617-626.

19. Phuong TT, Yun YH, Kim SJ, Kang TM. Positive feedback control between STIM1 and NFATc3 is required for C2C12 myoblast differentiation. *Biochem Biophys Res Commun*. 2013;430:722-728.

20. Sunadome K, Yamamoto T, Ebisuya M, Kondoh K, Sehara-Fujisawa A, Nishida E. ERK5 regulates muscle cell fusion through Klf transcription factors. *Dev Cell*. 2011;20:192-205.

21. Chandra G, Defour A, Mamchoui K, Pandey K, Mishra S, Mouly V, Sreetama S, Mahad Ahmad M, Mahjneh I, Morizono H, Pattabiraman N, Menon AK, Jaiswal JK. Dysregulated calcium homeostasis prevents plasma membrane repair in Anoctamin 5/TMEM16E-deficient patient muscle cells. *Cell Death Discov*. 2019;5:118.

22. Magri F, Del Bo R, D'Angelo MG, Sciacco M, Gandossini S, Govoni A, Napoli L, Ciscato P, Fortunato F, Brighina E, Bonato S, Bordoni A, Lucchini V, Corti S, Moggio M, Bresolin N, Comi GP. Frequency and characterisation of anoctamin 5 mutations in a cohort of Italian limb-girdle muscular dystrophy patients. *Neuromuscul Disord*. 2012;22:934-943.

23. Di Zanni E, Gradogna A, Scholz-Starke J, Boccaccio A. Gain of function of TMEM16E/ANO5 scrambling activity caused by a mutation associated with gnathodiaphyseal dysplasia. *Cell Mol Life Sci*. 2018;75:1657-1670.

24. Liu JH, König S, Michel M, Arnaudeau S, Fischer-Lougheed J, Bader CR, Bernheim L. Acceleration of human myoblast fusion by depolarization: graded Ca²⁺ signals involved. *Development*. 2003;130:3437-3446.